Targeting Faults for Geothermal Fluid Production: Exploring for Zones of Enhanced Permeability

Luke Mortimer[1,2], Adnan Aydin[3] and Craig T. Simmons[2]
[1]Hot Dry Rocks Pty Ltd, PO Box 251, South Yarra, Victoria 3141
[2]National Centre for Groundwater Research and Training, Flinders University, GPO Box 251, Adelaide, South Australia 5100
[3]Department of Geology and Geological Engineering, University of Mississippi, PO Box 1848, MS 38677, USA
luke.mortimer@hotdryrocks.com

Fault structures can potentially deliver increased geothermal fluid production by boosting the bulk permeability and fluid storage of a production zone. However, the hydromechanical properties of faults are inherently heterogeneous and anisotropic, thereby, making it challenging to distinguish between permeable and impermeable faults. This discussion paper outlines the key features that determine fault permeability and how the probability of locating zones of enhanced fault permeability can be derived from preliminary fault stress state modelling. It is proposed that preliminary fault stress state modelling for early stage exploration projects or in areas of unknown or complex geology can reduce the uncertainty and risk of exploring for fault-related geothermal targets.

Keywords: geothermal, exploration, fault, permeability, *in situ* stress, hydromechanical modelling.

Introduction

Permeable fault structures present an attractive geothermal exploration target as faults have been proven to boost substantially reservoir permeability and fluid production at some existing geothermal energy operations (e.g. Dixie Valley, USA; Landau, Germany). However, not all faults are permeable. Their hydraulic properties are inherently heterogeneous and difficult to characterize, making it challenging to distinguish between faults acting as fluid conduits and fluid barriers. This challenge is compounded when a fault has no surface expression because to achieve sufficiently high production fluid temperatures a fault typically must be intersected at some depth where the exact hydraulic character of the fault is unknown prior to drilling. Therefore, if exploring for permeable fault structures the key questions are: (1) which fault or fault segment has the highest probability of being permeable?; and (2) what information is required to reduce the uncertainty and exploration risk prior to drill testing? To help answer these questions the main objectives of this discussion paper are to describe the key features that determine fault permeability and how the probability of locating zones of enhanced fault permeability may be derived from preliminary fault stress state modelling. For illustrative purposes, hypothetical examples of preliminary fault stress state models are provided.

Targeting fault structures involves exploring at depth for zones of enhanced natural *in situ* fracture porosity and permeability to maximise geothermal fluid production from a prospective area. A permeable fault target can be viewed as either: (1) having sufficient natural *in situ* porosity and permeability with natural fluid recharge occurring at the optimal fluid temperature (e.g. Dixie Valley, USA); or (2) as a zone of enhanced porosity and permeability that may still require some degree of reservoir stimulation (e.g. Landau, Germany).

Two critical elements considered positive for fault permeability targets are:

(1) Favourable fault orientation with respect to the *in situ* stress field (i.e. 'critically stressed'); and

(2) Hydraulic contact with a significant volume of porous/fractured and permeable reservoir (i.e. fluid mass storage).

For the latter, the fluid mass storage may be provided by the fault structure itself or an adjoining and hydraulically connected rock unit such as thick, porous sandstone. Fluid overpressures associated with the fault may also be beneficial for fluid advection along the structure from a connected, deeper and potentially hotter reservoir and for lowering the effective stress state of the fault.

Fault Architecture and Hydrogeology

The architecture of a fault structure can vary greatly in form from simple faults where strain is accommodated along a narrow plane to more complex structures where strain is distributed over a composite zone that may include numerous faults, small fractures, veins, breccias and cataclastic gouge. Generally, fault structures are subdivided into two simple components being the fault core and the fault damage zone both of which may vary over widths ranging from centimetres to hundreds of metres (Figure 1; Caine and Forster, 1999; Gudmundsson *et al.*, 2009). These two components are distinguishable by their distinct mechanical and hydrogeological properties although these are inherently heterogeneous and can vary significantly along a fault. The fault core refers to the main fault plane that takes up most of the displacement and where

the original lithology has been altered through fault-related processes such as grain size reduction, hydrothermal alteration and mineral precipitation in response to mechanical and fluid flow processes (Caine and Forster, 1999). The character of the fault core zone is strongly dependent on its protolithology (Caine and Forster, 1999). Fault damage zones are defined as the adjacent network of subsidiary structures including small faults, fractures, veins, cleavage, pressure solution seams and folds that laterally decrease in density away from the fault core zone (Figure 1; Caine and Forster, 1999; Gudmundsson *et al.*, 2009)

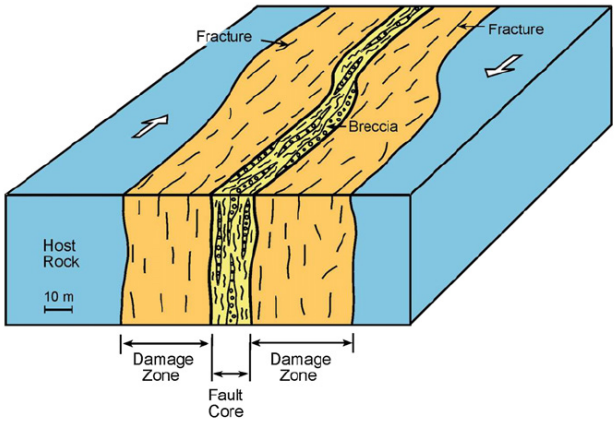

Figure 1. Illustrative schematic diagram of a fault including its fault core and damage zone. From Gudmundsson *et al.* (2009).

The permeability of faults can vary considerably ranging from impermeable flow barriers to significant flow conduits with a high degree of spatial heterogeneity and anisotropy. Generally, faulting in low porosity, competent rock is expected to result in an increase in fault zone permeability whilst faulting in high porosity sedimentary rocks may lead to a general decrease in fault zone permeability through communition and porosity reduction processes such grain-size reduction and the formation of clay-rich fault gouge and deformation bands (Zoback, 2007; Wong and Zhu, 1999). Commonly, fault cores are of a relatively lower permeability than their associated damage zones, which is attributed to porosity reducing processes occurring within the cores (Caine *et al.*, 2010). For example, at the Mirrors site, Dixie Valley geothermal field, measured core plug permeabilities ranged from 10^{-8} m^2 (10^7 mD) in fault damage zones to 10^{-20} m^2 (10^{-8} mD) in fault cores, however, the bulk permeability of the fault zone is on the order of 10^{-12} m^2 (1000 mD) (Caine and Forster, 1997; Seront *et al.*, 1998). In terms of anisotropy, the permeability tensor is expected to be at a maximum parallel to the fault, intermediate down dip of the fault plane and at a minimum perpendicular to the fault, which allows for both vertical and lateral flow but may limit cross-fault flow (Ferrill *et al.*, 2004). Faults of sufficiently high permeability can also contribute significantly to both local and regional scale coupled groundwater flow and heat transport via advection/convection processes (e.g. Bachler *et al.*, 2003).

Stress-Dependent Fault Permeability

Stress acting on a fault plane can be resolved into normal and shear stresses, which are the components of stress that act normal and parallel to a plane, respectively. In nature, these stresses are highly coupled and can cause faults to undergo reactivation and deform. The link between stress, fracture deformation and permeability is such that as fracture void geometries and the connectivity of a flow network change in response to changing *in situ* stress, the storage, permeability and flow pattern is also expected to change in magnitude, heterogeneity and/or anisotropy. Fracture deformation can result in significant changes in permeability and storage because the ability of a fracture to transmit a fluid is extremely sensitive to its aperture. For example, the transmissivity of an individual fracture (T_f) idealised as an equivalent parallel plate opening can be expressed as:

$$T_f = \frac{(2b)^3 \rho g}{12\mu} \qquad (1)$$

Where $2b$ is the fracture aperture width (m), ρ is the fluid density (kg.m^{-3}), g is gravitational acceleration (m.s^{-2}) and μ is the dynamic viscosity of the fluid (kg.m^{-2}.s).

One key aspect of exploring for permeable faults is the theory of stress-dependant fracture permeability in deep-seated, fractured rocks. This theory is supported by studies relating to hydrocarbon and geothermal reservoirs and studies of potential nuclear waste repository sites (e.g. Finkbeiner *et al.*, 1997; Gentier *et al.*, 2000; Hudson *et al.*, 2005). The theory is that *in situ* stress fields exert a significant control on fluid flow patterns in fractured rocks, particularly, for rocks of low matrix permeability. For example, in a key study of deep (>1.7 km) boreholes, Barton *et al.* (1995) found that permeability manifests itself as fluid flow focused along fractures favourably aligned within the *in situ* stress field, and that if fractures are critically stressed this can impart a significant anisotropy to the permeability of a fractured rock mass. Critically stressed fractures are defined as fractures that are close to frictional failure within the *in situ* stress field (Barton *et al.*, 1995). Specifically, the theory of stress-dependent fracture permeability predicts preferential flow occurring along fractures that are oriented orthogonal to the minimum principal stress (σ_3) direction (due to low normal stress), or inclined

~30° to the maximum principal stress (σ_1) direction (due to shear dilation).
Frictional sliding along a plane of weakness such as a fault occurs when the ratio of shear (τ) to the effective normal stress (σ'_n) equals or exceeds the frictional sliding resistance. It is based upon Amonton's Law, which governs fault reactivation:

$$\tau = \mu.\sigma'_n \quad (2)$$

Where μ is the coefficient of friction (a rock material property) and σ'_n is equal to the total applied normal stress resolved onto the plane minus the pore fluid pressure (i.e. $\sigma_n - P_P$). The value of μ has been found to typically range between 0.6 and 1.0 (Byerlee, 1978; Zoback, 2007). This relationship also shows that pore fluid pressure can have a significant impact as it determines the effective stress acting on a plane and that increasing pore pressures can de-stabilise a fault surface by increasing the ratio of shear to normal stress. The coupling of these hydromechanical (HM) processes means that fluid pressure and flow within faults is linked to tectonic stress and deformation through changes in permeability and storage whilst tectonic stress and deformation is linked to fluid flow through changes in fluid pressure and effective stress (NRC, 1996).

How exactly a fault will behave under an applied stress regime depends upon many factors, however, investigating stress-dependent fault permeability based solely on fault alignment with respect to the *in situ* stress field is an oversimplification. Just as important are the geomechanical properties of the host rock and its contained faults. Important intact rock material properties include parameters such as density, bulk moduli, uniaxial compressive strength, tensile strength, cohesion and friction angle that are typically estimated from laboratory tests. Fracture stiffness is a function of both fracture wall surface contact (i.e. fracture roughness profile) and the elastic properties of the intact rock material (i.e. bulk rock moduli) where for the same given alignment within an *in situ* stress field relatively stiff fractures deform less than weaker fractures. Fracture normal and shear stiffness are measures of resistance to deformation perpendicular and parallel to fracture walls, respectively, and both increase with increasing effective normal stress. In general, faults tend to exhibit high stiffness if formed within hard, competent rocks or if they become locked open by earlier deformation episodes (e.g. shear dislocation) or mineral infill and cementation, and may even become stress insensitive even if subjected to high effective normal stresses (Hillis, 1998; Laubach et al., 2004). In contrast, low stiffness faults can exhibit a wide range of shear and closure behaviour as their alignment with respect to σ_1 changes (Hillis, 1998). Ultimately, estimates of fracture stiffness attempt to account for more realistic fracture heterogeneity, asperity contact, deformation and tortuous fluid flow. Equations 3 & 4 below describe the simplified relationship between fracture stiffness and fracture deformation (Rutqvist and Stephannson, 2002):

$$\Delta\mu_n = jk_n \, \Delta\sigma'_n \quad (3)$$

$$\Delta\mu_s = jk_s \, \Delta\sigma_s \quad (4)$$

Which states (a) that fracture normal deformation ($\Delta\mu_n$) occurs in response to changes in effective normal stress ($\Delta\sigma'_n$) with the magnitude of opening or closure dependent upon fracture normal stiffness (jk_n); and (b) that the magnitude of shear mode displacement ($\Delta\mu_s$) depends upon the shear stiffness (jk_s) and changes in shear stress ($\Delta\sigma_s$).
Structural permeability within faults is likely to be a transient effect as faults often become modified by porosity reducing processes such as hydrothermal mineralisation, hence, fault deformation processes compete with permeability reduction caused by fluid flow (Sibson, 1996; Zoback, 2007). Active fault slip is typically episodic and can temporarily increase the permeability of a fault zone by as much as many orders of magnitude (Gudmundsson, 2000). Therefore, for faults to remain effective permeable structural conduits fault deformation processes must be at least intermittent to continual. For example, in the Dixie Valley geothermal field fluid production is sourced from high permeability faults and fractures that are favourably aligned and critically stressed whilst it is inferred that the formation of fault permeability associated with active deformation out competes permeability destroying hydrothermal quartz precipitation processes (Zoback, 2007).

Preliminary Modelling of Fault Stress States

The numerical modelling of fault stress states has previously been employed by several researchers to identify zones of potential fault enhanced permeability and fluid flux (e.g. Ferrill *et al.*, 2004; Gudmundsson, 2000; Moeck *et al.*, 2009; Zhang and Sanderson, 1996). In a similar methodology, this study uses the Universal Distinct Element Code (UDEC) to simulate the coupled HM response of deformable faulted rock masses under an applied *in situ* stress field to derive preliminary indications of fault stress states and, by corollary, their potential permeability. UDEC represents a rock mass as an assembly of discrete rigid or deformable, impermeable blocks separated by discontinuities (faults, joints etc) and can reproduce fully coupled HM behaviour (Itasca, 2004). Fluid pressure and fracture conductivity is dependent upon mechanical deformation whilst simultaneously fluid pressures

modify the mechanical behaviour of the fractures (for a comprehensive review of the UDEC governing equations see Itasca, 2004). The 2.5D UDEC models describe a geometrical reconstruction that consist of 2D horizontal planar or vertical slices of the conceptual faulted rock mass model and incorporates the effects of the 3D stress field (i.e. σ_V, σ_H, and σ_h). That is, the models perform plane strain analyses, which assumes that the model continues indefinitely (and uniformly) out of the plane of analysis with computations performed for a slice that is one unit thick (Itasca, 2004). The ultimate aim of this type of modelling is to distinguish which fault or fault segments in a specified area are critically stressed and, therefore, a potential exploration drill target. These models are designed to assist explorers in areas of unknown or complex geology prior to drilling, however, large model parameter uncertainties means that the results are preliminary indications only i.e. a 'probabilistic' representation of potential fault stress states.

To illustrate this methodology, three hypothetical geological models are presented based upon the northern Perth Basin as an example setting. This involves a strike-slip faulting stress regime, stress tensor $\sigma_H > \sigma_V > \sigma_h$ equivalent to 1.25 : 1.0 : 0.75 and an east-west principle horizontal stress (σ_H) orientation (King et al., 2008; van Ruth, 2006). For the purposes of this illustrative exercise, rock mass parameters (e.g. density, bulk modulus etc) were sourced from the UDEC rock property database although, where possible, these should be based upon measured representative field samples or at the very least global average values. The most difficult part of this process is assigning fault stiffness values, particularly, as they are expected to vary with host lithology. As fracture stiffness is a function of wall contact area, the jk_n for smooth planar surfaces can approximate the value of the Young's Modulus (*E*) whereas the jk_s, for perfectly matching rough surfaces, can approximate the value of the Shear Modulus (*G*). At shallow depths, estimates can be derived based upon jk_n ranging from 1/2 (smooth) to 1/10 (rough) the value of *E* and jk_s ranging from 1/2 (rough) to 1/10 (smooth) the value of *G*, which are compatible with published data and those derived from empirical relationships (Kulhawy, 1978; Norlund *et al*., 1995). However, prior to drill testing the true nature of the fault at depth is unknown. As the aim is to attempt to evaluate relative fault stress states, possibly across multiple faults and lithologies, a 'smooth' fault stiffness for each respective lithology was chosen along with zero tensile strength, cohesion and dilation angle values. In theory, these geomechanical properties replicate the behaviour of a 'weak' fault plane, which allows each fault segment to potentially deform. This is a reasonable approach as most active fault zones are inferred to be weak (Gudmundsson *et al.* 2001; Gudmundsson *et al.* 2009).

The three hypothetical geological model examples are:

Model 1: 4km x 4km horizontal planar model set at -3.5 km depth below the surface comprising of a single fault with jog hosted within sandstone (Figure 2).

Model 2: 5km x 5km cross-section of a listric fault hosted with a sedimentary sequence comprising of limestone (surface-1km depth), siltstone (1km-2.5km depth), shale (2.5km-3.5km depth), sandstone (3.5km-4km depth) and granite (4km–5km depth) (Figure 3).

Model 3: 4km x 4km horizontal planar model set at -3.5 km depth below the surface comprising of a central, circular, granite batholith of 1km radius hosted within a weak shale unit plus three cross-cutting faults of differing orientation (Figure 4).

In these models, rock mass deformation was defined by the Mohr-Coulomb model, which is the conventional model used to represent shear failure in rocks and soils whilst fracture behaviour was defined by the Coulomb-Slip criterion, which assigns elastic stiffness, tensile strength, frictional, cohesive and dilational characteristics to a fracture (Itasca, 2004). Mechanical boundaries were defined as fixed velocity (displacement) boundaries and initial *in situ* and boundary fluid pore pressures are assumed hydrostatic.

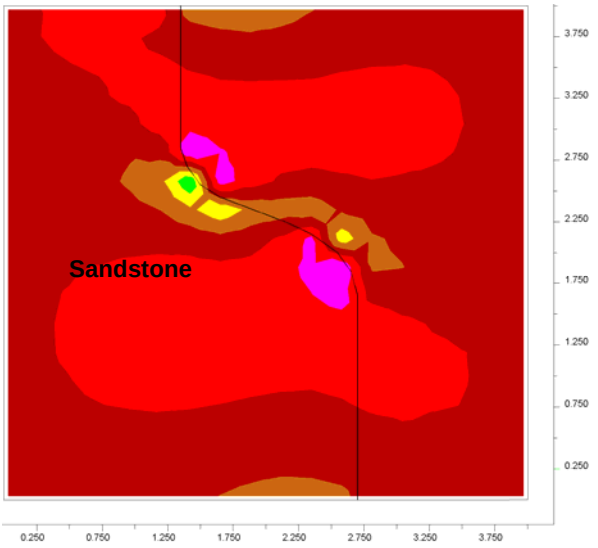

Figure 2. Model 1: 4km x 4km horizontal planar contour map of x-direction stress magnitudes highlighting the concentration of high and low stress zones into quadrants along the fault jog. This highlights that although fault alignment maybe favourable stress-dependent fault permeability can be segmented and localised. Note that the principle stress (σ_H) direction is east-west (right-left). Legend: purple, red, brown, green and yellow colours represent a decreasing range of high to low stress magnitudes, respectively.

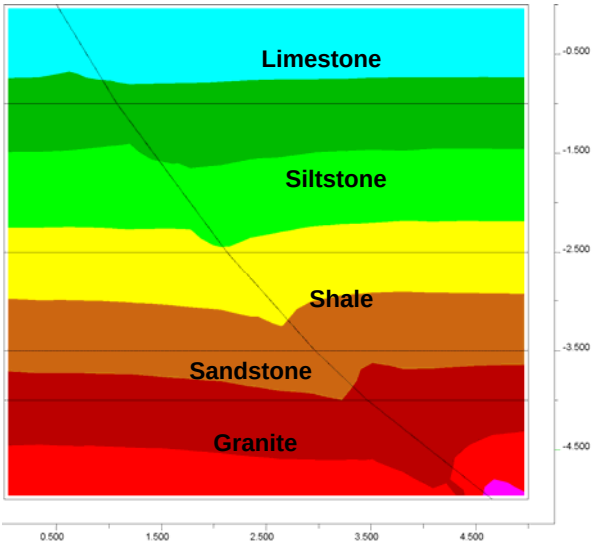

Figure 3. Model 2: 5km x 5km vertical cross-section profile of contoured y-direction stress magnitudes highlighting a localised low stress field perturbation closely associated with the trace of the listric fault. This indicates low fault plane stress and potentially enhanced fault permeability. Note that the principle stress (σ_H) direction is east-west (right-left). Legend: purple, red, brown, green and yellow colours represent a decreasing range of high to low stress magnitudes, respectively.

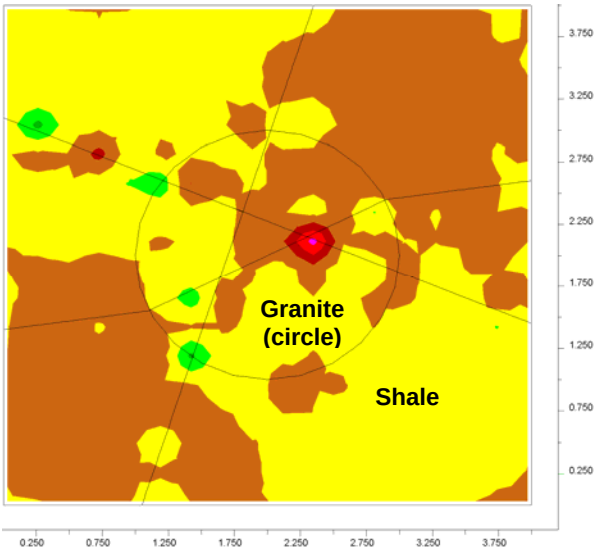

Figure 4. Model 3: 4km x 4km horizontal planar contour map of x,y-direction stress magnitudes highlighting a critically stressed fault intersection (red) which potentially represents the location of enhanced fault permeability. This intersection is also coincident with a low stress anomaly in the x- and y-direction. Note that the principle stress (σ_H) direction is east-west (right-left). Legend: purple, red, brown, green and yellow colours represent a decreasing range of high to low stress magnitudes, respectively.

Conclusion

The risks of targeting permeable faults as geothermal reservoirs include: (1) a relatively high permeability structure may result in fluid pathway short-circuiting and accelerated rates of reservoir thermal drawdown; (2) multiple fault structures with varying amounts of displacement may truncate and compartmentalise a reservoir thereby reducing accessible reservoir volume; and (3) the targeted fault structure may still be hydraulically sealed and/or stress insensitive as a result of other competing natural processes. These risks can be partially mitigated through interpretation of good quality seismic reflection data and with direct drill testing. The fault stress state models shown in this discussion paper are deliberately simplistic but specifically designed to demonstrate how this method can be used to identify zones of potentially enhanced fault permeability prior to any drill testing in areas of unknown or complex geology. This method may be of benefit to the Australian geothermal exploration sector as target depths are typically in excess of 3 km depth below the surface where natural *in situ* porosity and permeability are typically low and there is a general paucity of data.

Nevertheless, it is important to note that the results of such preliminary models can only indicate the probability of encountering enhanced fault permeability and that these 2D models simplify the 3D reality. It could be argued that simply evaluating targets on structural alignment relationships within the *in situ* stress field alone might be sufficient, however, in complex areas this would neglect the influence of features such as multiple rock competency and fault stiffness contrasts and fault intersections on perturbing the local stress field. The results of these numerical models are only as accurate as the quality of the input data and this particular methodology can include a significant amount of model parameter uncertainty (e.g. fault stiffness, estimated or inferred stress field etc). Therefore, this methodology should be viewed as just one tool that can form part of a broader exploration risk management strategy.

References

Bachler, D., Kohl, T., and Rybach, L., 2003, Impact of graben-parallel faults on hydrothermal convection-Rhine Graben case study: Physics and Chemistry of the Earth, 28, 431-441.

Barton, C.A., Zoback, M.D. and Moos, D., 1995, Fluid flow along potentially active faults in crystalline rock: Geology, 23, 683-683.

Byerlee, J.D., 1978, Friction of rocks: Pure and Applied Geophysics, 116, 615-626.

Caine, J.S. and Forster, C.B., 1997, Fault zone architecture and fluid flow. An example from Dixie Valley, Nevada: Proceedings 22nd Workshop on Geothermal Reservoir Engineering, Stanford University, Stanford, California.
Caine, J.S. and Forster, C.B., 1999, Fault zone architecture and fluid flow: insights from field data and numerical modelling, Faults and Subsurface Fluid Flow in the Shallow Crust: American Geophysical Union, Geophysical Monograph 113, 101-127.
Caine, J.S., Bruhn, R.L. and Forster, C.B., 2010, Internal structure, fault rocks and inferences regarding deformation, fluid flow, and mineralisation in the seismogenic Stillwater normal fault, Dixie Valley, Nevada: Journal of Structural Geology. In Press.
Ferrill, D.A., Sims, D.W., Waiting, J.W. Morris, A.P., Franklin, N.M. and Schultz, A.L., 2004, Structural framework of the Edwards Aquifer recharge zone in south-central Texas: GSA Bulletin, 116 (3/4), 407-418.
Finkbeiner, T., Barton, C.A. and Zoback, M.D., 1997, Relationships among in-situ stress, fractures and faults, and fluid flow: Monterey Formation, Santa Maria Basin, California: AAPG Bulletin, 81 (12), 1975-1999.
Gentier, S., Hopkins, D., and Riss, J., 2000. Role of Fracture Geometry in the Evolution of Flow Paths under Stress: *In* Faybishenko, B., Witherspoon, P.A and Benson, S.M. (eds), Dynamics of Fluids in Fractured Rocks. AGU Geophysical Monograph 122, 169-184.
Gudmundsson, A., 2000, Active faults and groundwater flow: Geophysical Research Letters, 27 (18), 2993-2996.
Gudmundsson, A., Berg, S.S, Lyslo, K.B. and Skurtveit, E., 2001, Fracture networks and fluid transport in active fault zones: Journal of Structural Geology, 23, 343-353.
Gudmundsson, A., Simmenes, T.H., Larsen, B. and Philipp, S.L., 2009, Effects of internal structure and local stresses on fracture propagation, deflection and arrest in fault zones: Journal of Structural Geology, In Press.
Hillis, R.R., 1998. The influence of fracture stiffness and the *in situ* stress field on the closure of natural fractures: Petroleum Geoscience, 4, 57-65.
Hudson, J. A., Stephansson, O., and Anderson, J., 2005. Guidance on numerical modelling of thermo-hydro-mechanical coupled processes for performance assessment of radioactive waste repositories: International Journal of Rock Mechanics and Mining Sciences, 42, 850-870.
Itasca, 2004. UDEC 4.0 Theory and Background. Itasca Consulting Group Inc., Minnesota.
King, R.C., Hillis, R.R., and Reynolds, S.D., 2008, In situ stresses and natural fractures in the Northern Perth Basin, Australia: Australian Journal of Earth Sciences, 55 (5), 685-701.
Kulhawy, F. H. and Goodman, R. E., 1980, Design of Foundations on Discontinuous Rock: Proceedings of the International Conference on Structural Foundations on Rock. International Society for Rock Mechanics, 1, 209-220.
Laubach, S. E., Olsen, J. E., and Gale, J. F. W., 2004. Are open fractures necessarily aligned with the maximum horizontal stress?: Earth and Planetary Science Letters, 222, 191-195.
Moeck, I., Kwiatek, G. and Zimmermann, G., 2009, Slip tendency analysis, fault reactivation potential and induced seismicity in a deep geothermal reservoir: Journal of Structural Geology, 31, 1174-1182.
National Research Council (NRC), 1996. Rock Fractures and Fluid Flow. Contemporary Understanding and Applications. National Academy of Sciences, Washington D.C.
Nordlund E, Radberg G, Jing L., 1995, Determination of failure modes in jointed pillars by numerical modelling: *In* Fractured and jointed rock masses. Balkema, Rotterdam, pp 345–350
Rutqvist, J. and Stephansson, O., 2003. The role of hydromechanical coupling in fractured rock engineering: Hydrogeology Journal, 11, 7-40.
Seront, B., Wong, T-F., Caine, J.S., Forster, C.B, Bruhn, R.L., and Fredrich, J.T., 1998, Laboratory characterisation of hydromechanical properties of a seismogenic normal fault system: Journal of Structural Geology, 20, 865-881.
Sibson, R.H., 1996, Structural permeability of fluid-driven fault-fracture meshes: Journal of Structural Geology, 18 (8), 1031-1042.
van Ruth PJ, 2006, Geomechanics: Vlaming Sub-Basin, Western Australia: CO2CRC Report Number RPT06-0043.
Wong, T-f. and Zhu, W., 1999, Brittle faulting and permeability evolution: hydromechanical measurement, microstructural observation, and network modeling, Faults and Subsurface Fluid Flow in the Shallow Crust: American Geophysical Union, Geophysical Monograph 113, 83-99.
Zoback, M. D., 2007. Reservoir Geomechanics. Cambridge University Press, New York, pp.449.
Zhang, X. and Sanderson, D.J., 1996, Numerical modelling of the effects of fault slip on fluid flow around extensional faults: Journal of Structural Geology, 18 (1), 109-119.

Acknowledgements

The authors gratefully acknowledge the funding and logistical support received for this research from the National Centre for Groundwater Research and Training, the Department of Water, Land and Biodiversity Conservation South Australia and the University of Hong Kong.